JOURNAL OF MATERIALS SCIENCE **38** (2003) 3597–3602

Characterization of the rust on carbon steels pre-corroded by different gaseous pollutants

YE WAN*, CHUANWEI YAN
State Key Laboratory for Corrosion and Protection, Institute of Metal Research, Chinese Academy of Sciences, Shenyang 110016, People's Republic of China
E-mail: ywan@imr.ac.cn

JUN TAN
Shenyang National Laboratory for Material Science, Institute of Metal Research, Chinese Academy of Sciences, Shenyang 110016, People's Republic of China

ZHI-MING SHI, CHU'NAN CAO
State Key Laboratory for Corrosion and Protection, Institute of Metal Research, Chinese Academy of Sciences, Shenyang 110016, People's Republic of China

Characterization of the rust formed during long-term atmosphere exposure at Beijing station on carbon steels pre-corroded by different gaseous pollutants was performed by means of Fourier transform infrared spectroscopy and X-ray diffraction. Goethite (α-FeOOH), Lepidocrocite (γ-FeOOH) and Feroxyhite δ-FeOOH are identified in the rust formed on all of the samples independent of the different pre-corrosion conditions and the different carbon steels. The results also show that: the rust constituent of the same kind of carbon steel pre-corroded by different pollutants are the same; the rust of carbon steels exposed for one year is some different to that exposed for two years; the phase constituents of the inner rust at the upper surface are the same as that at the downward surface, but those of the outer rust are different. It is concluded that the phase constituents of the rust of the same kind carbon steel after one year are the same under the different pre-corrosion conditions. © *2003 Kluwer Academic Publishers*

1. Introduction

Generally speaking, carbon steel always suffers from corrosion in ambient atmosphere before it is put into use, and the initial corrosion products may have some influence on the long-term exposure behavior.

An understanding of the atmospheric corrosion mechanism of steel requires a comprehensive study on the influence of environment on the formation of the rust. X-ray diffraction (XRD) can be useful for the characterization of the rust of carbon steels. However, in many occasions the phases of the rust are "amorphous", and they can hardly be identified by XRD [1]. Infrared absorption (IR) spectroscopy is one of the oldest and most commonly used techniques in chemistry to analyze the bonding characteristics among structural components in materials and can delineate various noncrystalline phases [2].

In this paper, carbon steels were pre-corroded in some artificial atmospheres containing certain such as sulfur dioxide, hydrogen sulfide or nitrogen dioxide for certain periods, then the pre-corroded samples and the blank samples were further exposed at Beijing station, located in the North part of China. Fourier transform infrared (FTIR) spectroscopy and XRD patterns of several representative rust products obtained from samples were used to characterize the phase constituents of the rusts and to deduce long-term corrosion performance.

2. Experimental methods

2.1. Preparation of specimens

Carbon steels A3 and 16Mn of chemical composition shown in Table I were studied, the steels were cut into plates with the dimensions of 100 mm × 50 mm × 4 mm, then mechanically polished, degreased, rinsed and dried. Some of the plates were pre-corroded in atmospheres with different gaseous pollutants for some days. The pre-corrosion parameters are list in Table II, with H_2S, NO_2 and SO_2 denoting the atmospheres contaminated by the respective gas, and damp air standing for air with 85%RH. Blanks in which specimens were not pre-corroded were also tested. The pollutants were provided by the Chinese National Research Center for Certified Reference Materials. The pre-corroded and blank plates were exposed for two years to a rural atmospheric environment (a Beijing's suburb) at an

---

*Author to whom all correspondence should be addressed.

0022–2461

TABLE I Nominal chemical composition of exposed carbon steels (wt%)

	C	S	P	Mn	Si	Al	Fe
A3	0.2	0.009	0.015	0.6	0.3		base
16Mn	0.16	0.025	0.009	1.4	0.4	0.05	base

TABLE II Pre-corroded parameter of exposed carbon steels

Pre-corrosion condition	Damp air	SO_2	H_2S	NO_2
Relative humidity (RH)	85%	85%	85%	85%
Temperature (°C)	35	35	35	35
Pollutant concentration (10^{-9})	–	11.3	33	206

angle of 45° to the ground facing south and under open condition.

2.2. Analysis of the rust

The surface morphology of the samples were caught by SONY DSC-F707, and the compactness of the samples was evaluated by Cambridge LEO S360 SEM photographs of cross-section.

The rust from the samples was characterized by means of FTIR spectroscopy and XRD. After one-year exposure, the rust products on the carbon steels were quite thick, and were possible to distinguish to be two different layers: outer and inner rust. The outer rust could be descaled very easily from the substrate (in some cases it could be separated as a whole using tweezers). The inner one was more adherent and carefully scraped off from the metallic substrate using a razor blade [1, 3]. The layers were then ground to fine powder with a mortar and pestle. A Nicolet Corporation model Magna-IR560 (with VeeMax accessory) infrared spectrophotometer was used to determine the spectra of the powdered samples, which were mixed evenly with spectrally pure KBr and pressed to form thin plates, then were subjected to infrared spectroscopic analysis by scanning 64 times in the spectral ranges 400 and 4000 cm^{-1} with spectral resolution of 8 cm^{-1}. The X-ray diffraction measurements were carried out using a model D/MAX-RB diffractometer with Cu K_α radiation and a scanning speed of 8° min^{-1} and 2θ was from 5° to 80°.

3. Result and discussion

A rust product was visible on the A3 and 16Mn steels after pre-corrosion in the atmospheres containing different gaseous pollutants. In order to study whether the preformed corrosion products were the same and whether the pre-corrosion conditions influence subsequent corrosion behavior, FTIR spectra of the pre-corroded samples were recorded. In the spectrum of the samples pre-corroded by the atmosphere containing NO_2, the peaks of NO_2^- and NO_3^- are evident, and the peaks of SO_3^{2-} and SO_4^{2-} are evident in the spectra of the samples pre-corroded by the atmospheres containing SO_2 and H_2S.

Whether the samples exposed at Beijing station for one year or two years, all of them corroded seriously. The FTIR spectra of carbon steel A3 pre-corroded by different gaseous pollutants were recorded to analyze any variation in the constituents of the rust. Fig. 1a shows the FTIR spectra of inner rust of steel A3 pre-corroded by the atmosphere contaminated with NO_2 and then outdoor exposed for 1 year. Although pre-corroded by NO_2-containing atmosphere, the peaks of NO_x^- were not detected. Fig. 1b, c and d show the FTIR spectra of the inner rust from one-year exposed samples pre-corroded in damp air, SO_2-containing atmosphere and H_2S-containing atmosphere, respectively, but S^{2-}, SO_3^{2-} or SO_4^{2-} was not detected on the corresponding samples.

It can also be seen from Fig. 1 that the FTIR spectra corresponding to different pre-corrosion conditions were similar. The powder-like, as well as the flake-like rust, formed on the steel surfaces consisted of a mixture of goethite (α-FeOOH), lepidocrocite (γ-FeOOH) and δ-FeOOH. Goethite had peculiar peaks at 885 cm^{-1}(s) and 780 cm^{-1}(s), and lepidocrocite

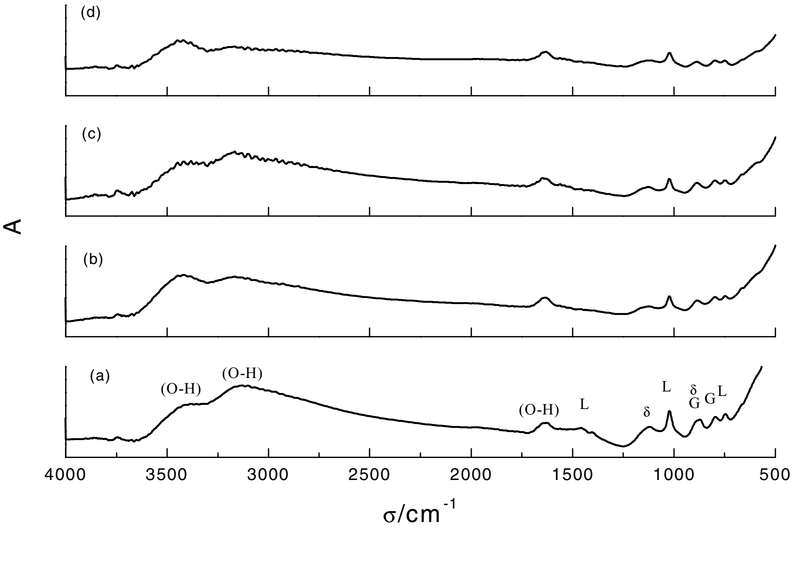

Figure 1 FTIR spectra of A3 steels pre-corroded by different pollutants ((a) NO_2, (b) damp air, (c) SO_2 and (d) H_2S) then exposed for 1 year at Beijing station. G: α-FeOOH, δ: δ-FeOOH, L: γ-FeOOH.

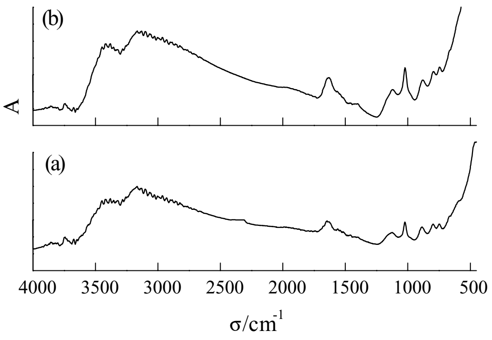

Figure 2 FTIR spectra of the inner rust of the samples pretreated by SO_2 then exposed 1 year (a) A3 steel, (b) 16Mn steel.

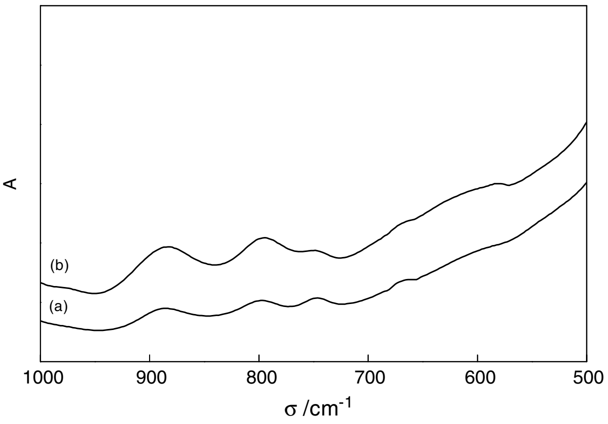

Figure 3 FTIR spectra of A3 steels pretreated by NO_2 and exposed for 1 year (a) FTIR spectra of the inner rust and (b) FTIR spectra of the outer rust.

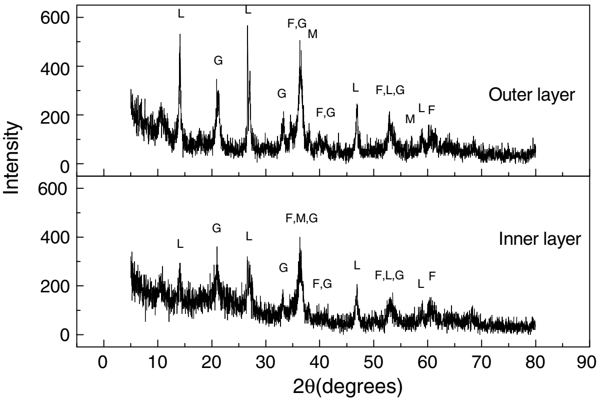

Figure 4 X-ray diffraction patterns of the outer and the inner layer rust of the 16Mn steel pretreated by SO_2 and exposed for 2 years (L: γ-FeOOH, G: α-FeOOH, F: $Fe_2O_3{\cdot}9H_2O$, M: γ-Fe_2O_3).

had peaks at 1020 cm^{-1}(s) and 750 cm^{-1}(vw) and 1450 cm^{-1}(vw), while the amorphous δ-FeOOH had peaks at 1124 cm^{-1}(mb) and 794 cm^{-1}(wb). Here, “s”, “vw” and “mb” stand for “strong”, “very weak” and “mild broad”, respectively. The FTIR spectra of the relevant phases can be found in the literature [2–4]. The peak at 3120 cm^{-1} is the O—H stretch vibration from lepidocrocite, and the peak at 3380 cm^{-1} is the O—H stretch vibration from δ-FeOOH [3, 5]. In addition, the absorption band found in the vicinity of 1640 cm^{-1} in Fig. 1 demonstrates that the rust contained a considerable amount of bound water.

After exposed for one year or two years, FTIR spectra of the inner layers from the samples pre-corroded under the same condition were similar, and the outer rust layers from the samples pre-corroded under the same condition were similar too. Fig. 2 shows the FTIR spectra of the inner rust of the different carbon steel samples pre-corroded in the SO_2-containing atmosphere and then exposed for one year. The spectra from the two kinds of carbon steels are similar. The frequencies of the main peculiar spectra are the same except the intensities are some different, therefore the main constituents of the rusts on the two kinds of carbon steels are the same and the content of every constituent is different.

After exposure for one year or two years, the inner and the outer rust on the same sample pre-corroded under the same condition had different FTIR spectra. Fig. 3 is the FTIR spectra recorded from A3 steel pre-corroded in the NO_2-containing atmosphere and then exposed for one year. The outer rust showed some difference from the inner rust. The analysis of the FTIR spectra of the different constituents indicates that goethite, lepidocrocite, δ-FeOOH, $Fe(OH)_3$ and magnetite, which spectra lies in 580 cm^{-1} and 745 cm^{-1} [6], are the constituents of the outer rust, of which the main difference with the inner rust is that the magnetite was not detected in the inner rust.

The XRD data were used to support the FTIR spectra results. Standards for the XRD analyses were obtained from literatures [4, 7–9]. Fig. 4 shows the XRD patterns of the outer and the inner rusts from carbon steel 16Mn pre-corroded in the SO_2-containing atmosphere and then exposed for two years. According to the XRD analysis results, the outer rust mainly consisted of the following phases: goethite (α-FeOOH: Joint Committee on Power Diffraction Standards [JCPDS] 290713), lepidocrocite (γ-FeOOH: JCPDS 80098), maghemite (γ-Fe_2O_3: JCPDS 391346) and ferrihydrite ($5Fe_2O_3{\cdot}9H_2O$: JCPDS 290712); while the inner rust was mainly made up of goethite, lepidocrocite and ferrihydrite. The lines corresponding to goethite, lepidocrocite and ferrihydrite were clearly identified in both of the XRD patterns recorded from the inner and the outer rusts. The relative intensities of goethite in the inner rust layer were stronger than those in the outer layer, and the diffraction peaks of the inner rust were broader than those in the outer rust. This latter result indicates that the grain size of the inner layer rust was smaller than that of the outer layer. Rust with a smaller grain size may more compact and therefore may more effectively hinder the inward permeation of water and oxygen and hence retard further corrosion of the samples.

From the XRD patterns (Fig. 5) of the rust layers formed on steel A3 after pre-corrosion in the SO_2-containing atmosphere followed by 1 year exposure, it can be seen that goethite, lepidocrocite, ferrihydrite and maghemite are the main oxides identified in each layer. Besides the four constituents, the diffraction peaks due to the magnetite are clearly identified in the outer rust in Fig. 5. It can also be seen from Fig. 5 that the relative peak intensities with the corresponding peaks of

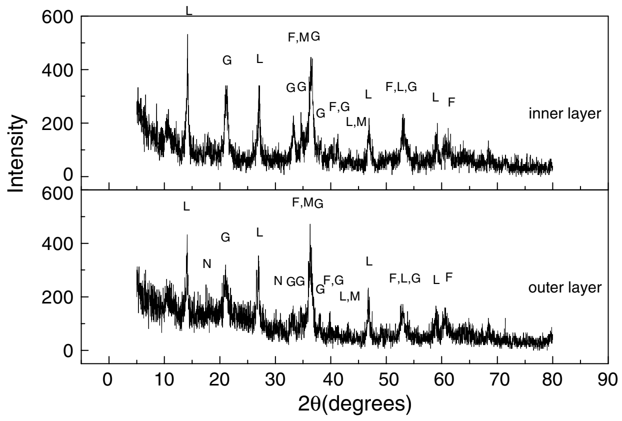

Figure 5 X-ray diffraction patterns of the outer layer and the inner layer corrosion products of the A3 steel pretreated by SO_2 and exposed for 2 years (L: γ-FeOOH, G: α-FeOOH, F: $Fe_2O_3 \cdot 9H_2O$, M: γ-Fe_2O_3, N: Fe_3O_4).

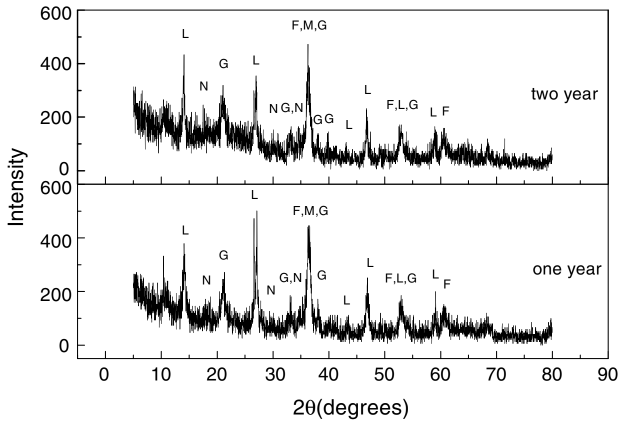

Figure 6 X-ray diffraction patterns of the outer layer rust of the A3 steel pretreated by SO_2 and exposed for 1 year and 2 years (L: γ-FeOOH, G: α-FeOOH, F: $Fe_2O_3 \cdot 9H_2O$, M: γ-Fe_2O_3, N: Fe_3O_4).

goethite and lepidocrocite were very different. The relative peak intensities of lepidocrocite in the outer rust layer were much stronger than those in the inner rust layer.

The XRD patterns of the samples exposed for one year and two years were similar independent of the pre-corrosion conditions. Fig. 6 shows that the XRD patterns of the outer rust of steel A3 pre-corroded in the SO_2-containing atmosphere and then exposed for one year and two years. The phase constituents in both of the XRD patterns were mainly identified to be goethite, lepidocrocite, maghemite, ferrihydrite and magnetite. The relative peak intensities of goethite in the pattern of the sample exposed for two years are higher than that for one year, while the relative peak intensities of lepidocrocite are lower than that for one year. It has been proposed [10, 11] that lepidocrocite can be transformed into goethite by a solid state transformation. A possible explanation for those observations is that lepidocrocite tends to transform into goethite in the inner rust, and the fine goethite possesses the cation selective ability that impedes the penetration of aggressive anions passing through the rust layer to the steel surface [12].

The XRD patterns of the inner rust of steel A3 pre-corroded in the SO_2-containing atmosphere and then exposed for one year and two years were similar too, and the phase constituents were mainly goethite, lepidocrocite, maghemite and ferrihydrite. Just as the outer rust, the relative peak intensities of goethite of the inner rust of the samples exposed for two years were higher than that for one year, while the relative peak intensities of the lepidocrocite were lower than that for one year. Thus it may be concluded that lepidocrocite tends to transform into goethite in the two layers of the rust.

It can be seen from the XRD patterns that goethite and lepidocrocite were the main constituents, which are in agree with the result from the FTIR spectra. δ-FeOOH was also the main constituent. The peaks of δ-FeOOH were mixed with that of goethite and lepidocrocite in the XRD patterns, while the peaks of the three phases can be clearly identified in the FTIR spectra. The pre-corrosion conditions had no influence on the long-term atmospheric corrosion products of the two kinds of carbon steels.

During the following exposure, it was found that the downward surface corroded more seriously and had a looser rust layer than the upward surface, as was shown in Figs 7 and 8. During the exposure, the upward surface was shined in the sun and was easy to be dried, and the precipitation and the rust could be washed down by rainfall; while the downward surface had a longer time of wetness, which caused more serious corrosion than the upward surface. It can be seen from Fig. 8a and c that the rust was made up of two layers and the downward surface of A3 steel is looser than that of 16 mn steel. The upward surface morphology of 16 mn steel is the same as that of A3 steel. The outer layer is looser and easier to fall off from the samples than the inner, and this is the reason why the cross-section photograph showed only a layer and why the downward rust was brownish yellow and the upward rust was brownish black. The inner rust is more compact and therefore the inner rust may more effectively hinder the inward permeation of water and oxygen and hence retard further corrosion of the samples, which is in agreement with the results from the XRD.

Table III is the corrosion rates of the carbon steels exposed for one year and two years. The corrosion rates of steel A3 are greater than those of steel 16Mn pre-corroded under the same pre-corrosion conditions. Table I shows that the chemical compositions of steel A3 and steel 16Mn are different. Aluminum is present in steel 16Mn and absent in steel A3, while the content of manganese in steel 16Mn is higher than that of steel A3. Aluminum can combine with other elements into inclusions that are hard to melt and disperse in the steel, which makes the crystal grain of steels finer [13] and improve the anti-corrosion of steels [14]. Iron sulfide always arranges along the crystal boundary and makes steel brickle, and manganese is a desulfurizer and a deoxidizing agent in steels. After manganese desulfurizes from iron sulfide, manganese sulfide will be formed and will avoid sulfur arrange along the crystal boundary, besides manganese can make pearlite finer [15]. Other than this, Sulphide inclusions are inactive as sites for

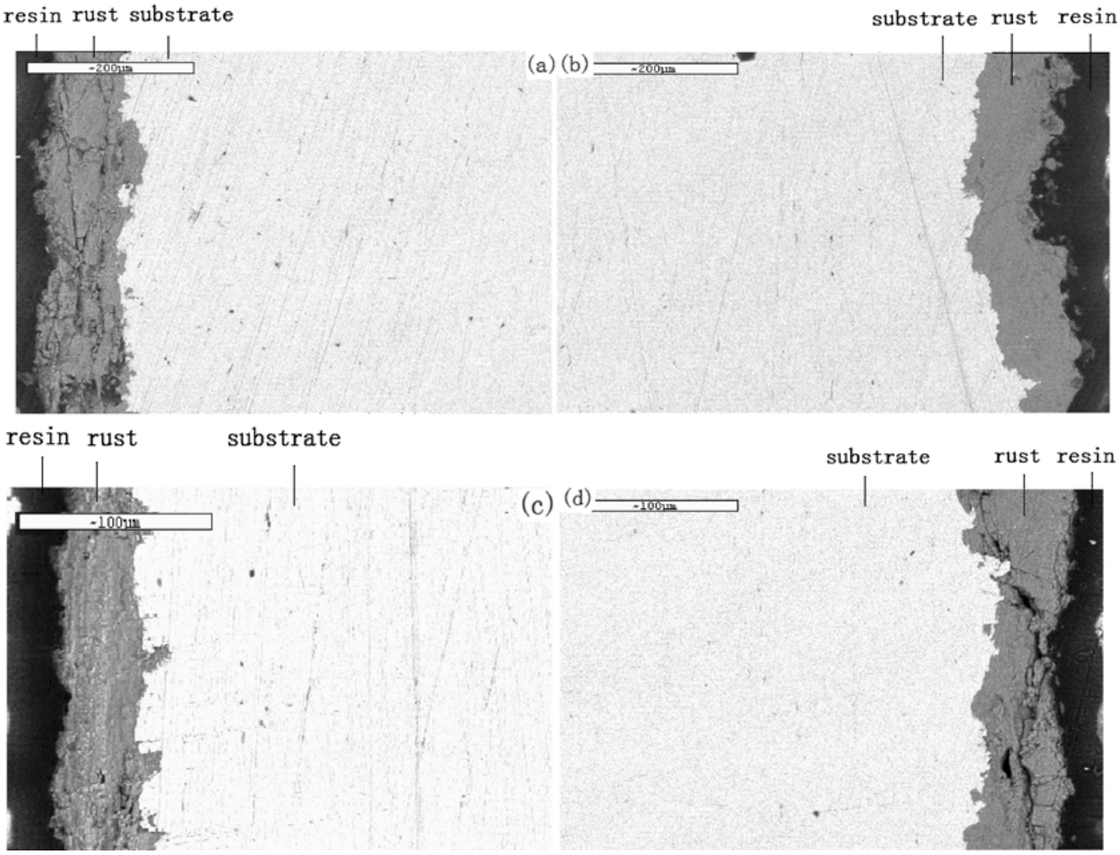

Figure 7 Cross-section photographs of the samples exposed for 1 year. (a) the downward rust of A3 steel, (b) the upward rust of A3 steel, (c) the upward rust of 16Mn steel, and (d) the downward rust of 16Mn steel.

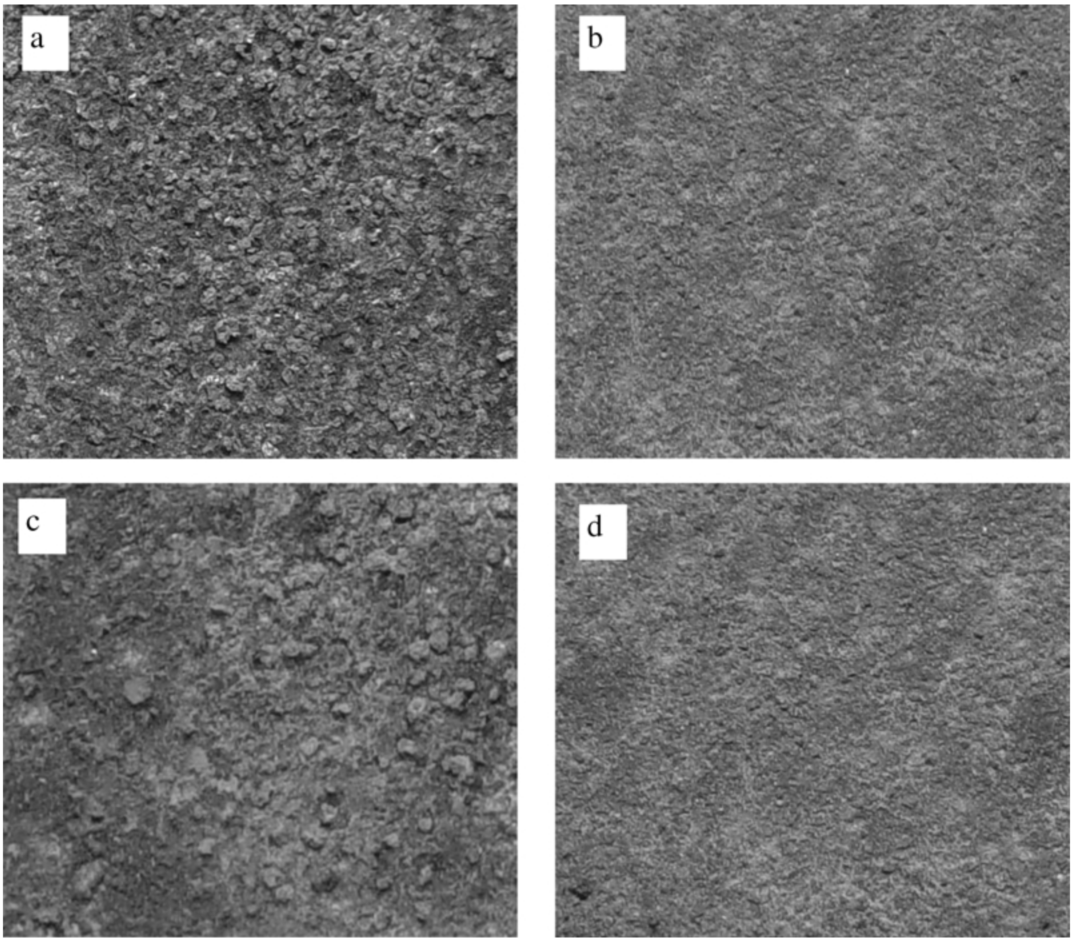

Figure 8 Morphology of the sample exposed for 1 year (a) the downward surface of A3 steel, (b) the upward surface of A3 steel, (c) the downward surface of 16Mn steel, and (d) the upward surface of 16Mn steel.

TABLE III Corrosion rates of carbon steels, μm/a

Pre-corrosion condition	Damp air		H_2S		NO_2		SO_2		Blank	
Time (a)	1st	2nd	1st	2nd	1st	2nd	1st	2nd	1st	2nd
16Mn	37.2	8.8	37.7	10.3	38.4	7.5	37.2	10.6	37.9	9.8
A3	40.2	9.2	40.3	12.3	41.5	9.9	40.8	10.4	41.2	9.6

stable corrosion initiation if they are sufficiently small. This is because a small open cavity formed by the initial triggering cannot retain a solution of composition that is sufficiently aggressive to continue the corrosion [16]. Therefore 16Mn steel corroded lighter than A3 steel because of the correlation of aluminum and manganese.

It can be seen from Table III that the corrosion rates of the first year were much greater than those of the second year. This is because the rust formed in the first year hinders the corrosive medium to permeate inward and hence retards further corrosion of the samples in the second year. The corrosion rates of the samples pre-corroded by NO_2 in the first year are the greatest, followed by blank, H_2S, SO_2 and damp air, while the corrosion rates of the samples in the second year and pre-corroded by NO_2 is lighter than those by other atmospheres. NO_2 triggered corrosion of the samples during the pre-corrosion. This effect is caused primarily by electrochemical reduction of NO_2 on the surface of the steels, the formation of nitrite shows that NO_2 reduction is contributing to the cathodic current on the surface [17] [reaction (1)–(4)]. The corrosion effects of SO_2 and H_2S are their hydrolyzations [reaction (5)–(9)]. Thus the corrosion rates of the samples pre-corroded by NO_2 are greater than by other atmospheres. The pre-corrosion products activated the samples' corrosiveness in the first year. After the active corrosion products were depleted by the environmental factors, the corrosion rates of the samples pre-corroded by NO_2 will be smaller than others.

$$NO_2\ (g) \Leftrightarrow NO_2\ (ads) \qquad (1)$$

$$3NO_2\ (ads) + H_2O \rightarrow 2NO_3^-\ (ads) + NO\ (g) + 2H^+\ (ads) \qquad (2)$$

$$NO_2\ (g) + e \rightarrow NO_2^-\ (ads) \qquad (3)$$

$$NO_2^-\ (ads) \Leftrightarrow H^+ + NO^-\ (ads) \qquad (4)$$

$$SO_2\ (g) \Leftrightarrow SO_2\ (aq) \qquad (5)$$

$$SO_2\ (aq) + H_2O \Leftrightarrow HSO_3^-(aq) + H^+\ (aq) \qquad (6)$$

$$HSO_3^-\ (aq) + {}^1\!/_2O_2^+\ (aq) \rightarrow SO_4^{2-}(aq) + H^+\ (aq) \qquad (7)$$

$$H_2S\ (g) \Leftrightarrow H_2S\ (aq) \qquad (8)$$

$$H_2S\ (aq) \Leftrightarrow S^{2-}\ (aq) + 2H^+\ (aq) \qquad (9)$$

$$M + xH_2O \rightarrow M \cdot xH_2O + ne^- \qquad (10)$$

$$O_2 + 2H_2O + 4e^- \rightarrow 4OH^- \qquad (11)$$

The local environment of the blank samples and the samples in the damp air is acidified by the hydrolysis of the dissolving metal (M) cations [reaction (10)–(11)]. Thus their corrosion rates are smaller than the samples pre-corroded by the other atmospheres.

4. Conclusions

1. The inner or the outer rusts of carbon steels pre-corroded by different atmospheres were similar, and phase constituents of the rust are mainly goethite, lepidocrocite and δ-FeOOH regardless of the pre-corrosion conditions.

2. The inner rusts of two kinds of carbon steel exposed for one year and two years were similar, while the outer rust for one year and two years had some differences. Lepidocrocite tends to transform into goethite in both of the outer and the inner rusts.

3. The phase constituent of the rusts of carbon steel A3 and carbon steel 16Mn were different, and this might be the reason that carbon steel A3 corroded more serious than carbon steel 16Mn.

Acknowledgements

This project was supported by the National Natural Science Foundation of China (No. 59899144). Exposure tests were carried out through cooperation with Institute of Aeronautical Materials, Beijing.

References

1. J. F. MARCO, M. GRACIA, J. R. GANCEDO, M. A. MARTÍNLUENGO and G. JOSEPH, *Corros. Sci.* **42** (2000) 762.
2. A. RAMAN, B. KUBAN and A. RAZVAN, *ibid.* **32**(12) (1991) 1295.
3. M. YAMASHITA, H. MIYUKI, Y. MATSUDA, H. NAGANO and T. MISAWA, *ibid.* **36**(2) (1994) 291.
4. T. MISAWA, K. ASAMI, K. HSHIMOTO and S. SHIMODAIRA, *ibid.* **14** (1974) 279.
5. J. G. WU, in "Techniques and Applications of Infrared Fourier Transform spectroscopy" (Science and Technology Information Press, Beijing, 1994) Vol. 2, p. 271.
6. R. A. NYQUIST and R. O. KAGEL, in "Infrared Spectra of Inorganic Compounds" (Academic Press, New York and London, 1971) p. 219.
7. T. NISHIMURA, H. KATAYAMA, K. NODA and T. KODAMA, *Corros.* **56**(9) (2000) 936.
8. J. F. MARCO, M. GRACIA, J. R. GANCEDO, M. A. MARTINLUENGO and G. JOSEPH, *Corros. Sci.* **42** (2000) 762.
9. S. J. OH, D. C. COOK and H. E. TOWNSEND, *ibid.* **41** (1999) 1690.
10. T. MISAWA, K. ASAMI, K. HASHIMOTO and S. SHIMODAIRA, *ibid.* **14** (1974) 131.
11. *Idem.*, *ibid.* **14** (1974) 279.
12. M. YAMASHITA and H. UCHIDA, *Hyperfine Interactions* **139**(140) (2002) 154.
13. Z. B SUN, P. F Z, H. G. LIN and T. S. YU, in "Handbook of Alloy Steel" (Metallurgy and Industry Press, 1982) Vol. 1, p. 62.
14. *Idem.*, in "Handbook of Alloy Steel" (Metallurgy and Industry Press, 1982) Vol. 1, p. 66.
15. *Idem.*, in "Handbook of Alloy Steel" (Metallurgy and Industry Press, 1982) Vol. 1, p. 55.
16. M. P. RYAN, D. E. WILLIAMS, R. J. CHATER, B. M. HUTTON and D. S. MCPHAIL, *Nature* **415**(14) (2002) 772.
17. J. E. SVENSSON and L. G. JOHANSSON, *Corros. Sci.* **34**(5) (2000) 736.

Received 17 September 2002
and accepted 10 June 2003